

Lifetime Measurements of Superdeformed Bands in $^{148-149}\text{Gd}$ and ^{152}Dy : Evidence for Structure-Dependent Elongations

H. Savajols,¹ A. Korichi,² D. Ward,³ D. Appelbe,⁴ G. C. Ball,³ C. Beausang,⁴ F. A. Beck,¹ T. Byrski,¹ D. Curien,¹ P. Dagnall,⁵ G. de France,¹ D. Disdier,¹ G. Duchêne,¹ S. Erturk,⁴ C. Finck,¹ S. Flibotte,^{3,6} B. Gall,¹ A. Galindo-Uribarri,³ B. Haas,¹ G. Hackman,⁶ V. P. Janzen,³ B. Kharraja,¹ J. C. Lisle,⁵ J. C. Merdinger,¹ S. M. Mullins,⁶ S. Pilotte,¹ D. Prévost,¹ D. C. Radford,³ V. Rauch,¹ C. Rigollet,¹ D. Smalley,⁵ M. B. Smith,⁴ O. Stezowski,¹ J. Styczen,⁷ Ch. Theisen,¹ P. J. Twin,⁴ J. P. Vivien,¹ J. C. Waddington,⁶ K. Zuber,⁷ and I. Ragnarsson⁸

¹Centre de Recherches Nucléaires, IN2P3-CNRS/Université Louis Pasteur, F-67037 Strasbourg Cedex 2, France

²Institut de Physique Nucléaire, IN2P3-CNRS, Bât.104, F-91406 Orsay Cedex, France

³AECL, Chalk River Laboratories, Chalk River, Ontario, Canada KOJ 1J0

⁴Oliver Lodge Laboratory, University of Liverpool, Liverpool L693BX, United Kingdom

⁵Schuster Laboratory, University of Manchester, Manchester M139PL, United Kingdom

⁶Department of Physics and Astronomy, McMaster University, Hamilton, Ontario, Canada L8S 4M1

⁷Institute of Nuclear Physics, PL31-342, Krakow, Poland

⁸Department of Mathematical Physics, Lund Institute of Technology, Box 118, S-221 00 Lund, Sweden

(Received 7 November 1995)

Precise level lifetimes have been measured for various superdeformed bands in $^{148,149}\text{Gd}$ and ^{152}Dy with the Doppler-shift attenuation method. From the derived quadrupole moments, Q_0 , we find large differences in deformation between the yrast bands and some excited bands in the gadolinium isotopes. Moreover, two of the excited Gd bands and the ^{152}Dy yrast band, which have identical moments of inertia, have different elongations, supporting the picture that alignment and deformation effects cancel in identical bands. [S0031-9007(96)00390-0]

PACS numbers: 21.10.Re, 21.10.Ky, 21.10.Tg, 27.70.+q

The existence of superdeformed (SD) rotational bands in atomic nuclei is related to the presence of a second minimum in the potential energy surface. This minimum, associated with very elongated ellipsoidal shapes corresponding to an axis ratio of roughly 2 : 1, is stabilized by shell gaps in the single-particle energy spectrum. The gaps remain even when the nucleus is rotated, except for a few high- j , high- N (N being the principal oscillator number) "intruder" orbitals which are brought close to the SD Fermi level by a combination of the large deformation and high rotational frequency. In the mass $A \sim 150$ region, the dynamical moments of inertia $J^{(2)}$ of yrast SD bands show significant variations with particle number, and the observed changes have been attributed to different occupations of the high- N intruder orbitals [1,2]. These states, i.e., $N = 7$ neutrons and $N = 6$ protons, carry large intrinsic quadrupole moments and therefore lead to shape-polarization effects causing deformation variations between the various SD bands: the more high- N intruder orbitals occupied, the greater the elongation. Such changes in deformation can, in principle, be derived from the quadrupole moments of the bands, which, in turn, can be extracted from lifetime measurements. Around the proton $Z = 66$ and neutron $N = 86$ SD shell gaps, measurements have been performed for the yrast SD bands in $^{152-153}\text{Dy}$ [3,4] and $^{149-150}\text{Gd}$ [5,6], and the results have shown that these bands are indeed associated with a large elongation, but, because of the uncertainties, no conclusion could be drawn concerning possible differences in deformation.

Many excited SD bands are known in this mass region. However, because of their weaker intensities compared to the yrast SD structures, lifetime measurements were not possible until now. Such experiments are even more crucial since the remarkable discovery of pairs of identical bands (IBs) with almost identical $J^{(2)}$ values (less than 0.3% difference) in nuclei which differ by one to four mass units [7]. Various models have been used and different mechanisms have been proposed in explanation, but none is fully satisfactory. To put more restrictive constraints on theoretical models, it is important to investigate if identical bands also have the same elongations.

The present work is devoted to the study of SD bands in gadolinium and dysprosium isotopes. Six SD bands, with very different $J^{(2)}$ moments, are known in ^{149}Gd [8] and in ^{148}Gd [9,10]: the yrast band labeled band 1 and five excited bands labeled 2 to 6. Several of these excited bands are IBs, for example, $^{149}\text{Gd}(4)$ and $^{148}\text{Gd}(5)$ have nearly the same $J^{(2)}$ as $^{152}\text{Dy}(1)$. By measuring accurately the level lifetimes of SD bands in these isotopes, we can investigate whether the predicted deformation changes associated with different single-particle configurations do indeed exist. Furthermore, a precise quadrupole moment determination of the yrast SD band in ^{152}Dy will enable us to establish the deformations associated with IBs in nuclei differing by 3 and 4 mass units. Since, in our experiments, the initial recoil velocities of the ions and stopping media were either identical or very similar, there will be cancellation of

some systematic errors, such as the uncertainty in the stopping powers, when relative Q_0 values are compared.

The $^{148-149}\text{Gd}$ residues were produced via the $^{124}\text{Sn} + ^{30}\text{Si}$ fusion reaction after evaporation of six and five neutrons, respectively. The energy of the silicon beam, delivered by the CRN Strasbourg Vivitron accelerator, was 158 MeV. The target consisted of 1.0 mg/cm^2 ^{124}Sn backed with 15 mg/cm^2 of gold. In order to prevent migration of the tin atoms into the gold backing due to target heating caused by the beam, it was essential to use an evaporated aluminum layer ($\sim 50 \mu\text{g/cm}^2$) as a buffer. In-beam γ rays were detected with the Eurogam II array [11]. The measurements described here were performed with a total of 54 Compton-suppressed germanium (Ge) detectors, 30 tapered coaxial Ge detectors from Eurogam I located in the forward and backward hemispheres, and 24 clover detectors installed at $\sim 90^\circ$ relative to the beam axis. The number of Ge crystals at each angle with respect to the beam direction is (5, 22°), (10, 46°), (24, 71°), (24, 80°), (24, 100°), (24, 109°), (10, 134°), and (5, 158°). Coincidence events were recorded only when the number of Ge detectors fired (ignoring the suppression signals) was greater than six. A total of 1.4×10^9 Compton-suppressed fourfold and higher-fold coincidence events were recorded. Under the same experimental conditions, we have investigated the yrast SD band in ^{152}Dy using the $^{120}\text{Sn}(^{36}\text{S}, 4n)$ reaction at an incident energy of 170 MeV and collecting approximately 2×10^8 coincidence events.

The lifetimes of SD states in rare-earth nuclei are expected to be less than 200 fs [3], and hence the γ rays connecting these states will be Doppler shifted. The observed shifts were divided by the full Doppler shift to generate the fractional shifts (F factors) which are shown in Fig. 1 as a function of the energy of the SD γ -ray transitions. The full shift was calculated with the bombarding energy at the midpoint of the target layer, assuming that the evaporated neutrons did not perturb the average speed of the fused system. The fact that the observed F values closely approach unity at the top of the bands substantiates the experimental method, since we would not expect significant time delays in feeding the highest observed SD states. An observed F value represents the average recoiling velocity and hence mean time at which a particular nuclear state decayed. But to extract a lifetime of a state it is necessary to know the average time, or time history, over which it was populated. The problem simplifies if most of the population of a level proceeded from an observed state. This is the case for SD bands in the so-called plateau region (the spin region where the relative intensities of the SD band members are $\approx 100\%$). In the region where unobserved feeding occurs, i.e., at spins above the plateau, the unknown time history presents a serious, but nevertheless tractable, problem. To calculate F values, we assumed feeding into each SD state by a rotational band according to the experimentally observed intensity

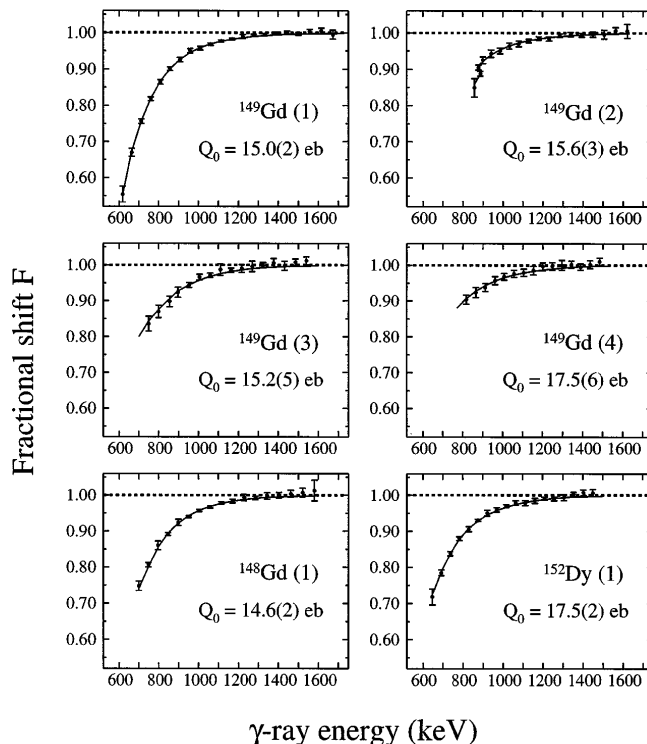


FIG. 1. Measured fractional shifts F for SD bands in $^{148,149}\text{Gd}$ and ^{152}Dy together with the calculated fractional shifts for a constant in-band quadrupole moment indicated in each panel (see text). Centroid shifts were determined by comparing γ -ray triple-gated coincidence spectra measured at $\theta = 22^\circ$ and 158° or $\theta = 46^\circ$ and 134° . The measured F values were obtained from double-gated γ -ray spectra in the case of $^{152}\text{Dy}(1)$. Various sets of gates have been tested. For example, to determine the F factors at very high spin, only transitions in the plateau region were selected. Alternatively, the F factors at lower spin were obtained with gates set only on transitions in the feeding region. It turns out that the extracted F values are very similar, and the curves shown were obtained from a set of gates comprising all transitions.

values. These bands had a common moment of inertia, and their intrinsic quadrupole moment $(Q_0)_{\text{SF}}$ could be varied from band to band.

The slowing-down history of the recoiling nuclei was treated by two different but standard techniques. In the first method we considered five trajectories sampling the target layer and took the unweighted average F values. Electronic stopping powers for gadolinium or dysprosium ions in tin, aluminum, and gold materials were taken from the Northcliffe and Schilling tables [12], scaled according to experimental values for ^4He ions as suggested by Sie *et al.* [13]. The nuclear contribution to the stopping power was taken from the theory of Lindhard, Scharff, and Schiott [14] as parametrized by Winterbon [15]. Multiple scattering was taken into account in an approximate way with the treatment of Blaugrund [16]. The second method for calculating the slowing down history used the code of Bacelar *et al.* [17], as modified by Gascon

et al. [18]. Electronic stopping was calculated according to the compilation by Ziegler, Biersack, and Littmark [19], and the code used Monte Carlo techniques to treat nuclear scattering processes according to the cross section of Lindhard, Scharff, and Schiott [14]. This method allowed events to be initiated uniformly over the target layer. The agreement between the two methods was excellent.

The analysis of the decay curves proceeded from the top of the bands. The free in-band and side-feeding quadrupole moment parameters $(Q_0)_B$ and $(Q_0)_{SF}$ were varied in a two-dimensional minimization of χ^2 for the F values in a particular band. Assuming the validity of the rotational model, the partial decay rate t (in ps^{-1}) of a band member with spin I can be written

$$t(I \rightarrow I - 2) = 1.22E_\gamma^5 Q_0^2 (IK20 | (I - 2)K)^2, \quad (1)$$

where E_γ is the γ -ray energy in MeV and Q_0 is expressed in e barn.

For all bands analyzed in the present work, we find that good fits to the data can be obtained with a single value for $(Q_0)_B$, except for the lowest spin state in bands 1 and 2 in ^{149}Gd . The quadrupole moment values are reported in Table I, and the quoted statistical errors include the covariance between $(Q_0)_B$ and $(Q_0)_{SF}$. Concerning the yrast band in ^{149}Gd , there is a sharp discontinuity in Q_0 for the last state which deexcites via a 617 keV transition ($Q_0 \approx 8 e b$), and a similar drop of collectivity occurs in band 2 after the backbending observed at low frequency (see Fig. 1). For $^{149}\text{Gd}(1)$ and $^{148}\text{Gd}(1)$, the fits can be improved if we allow Q_0 for the lowest three levels (excluding the state deexciting via the 617 keV γ -ray transition in ^{149}Gd) to be $\sim 10\%$ larger than the average for the whole band. However, the solidity of this result depends on a very detailed analysis of experimental uncertainties, in particular, the choice of

TABLE I. Q_0 quadrupole moment values (in $e b$) derived for SD bands in $^{148,149}\text{Gd}$ and ^{152}Dy compared with calculated values, Eq. (2), at spin $I \approx 40\hbar$. In the last column, the values have been scaled by a factor of 0.92. The quoted errors do not include stopping power uncertainties. Notice that, due to possible differences in the stopping powers ($\sim 2\%$) when comparing relative Q_0 values for ^{152}Dy and $^{148,149}\text{Gd}$ (same stopper but different recoiling ions), the error on Q_0 for ^{152}Dy should be increased to $0.3 e b$.

		Q_0 (exp)	Q_0 (calc)	$0.92Q_0$ (calc)
^{149}Gd	Band 1	15.0 (2)	16.5	15.2
	Band 2	15.6 (3)	16.7	15.4
	Band 3	15.2 (5)	17.4	16.0
	Band 4	17.5 (6)	19.3	17.7
^{148}Gd	Band 1	14.6 (2)	16.0	14.7
	Band 2	14.8 (3)	16.0	14.7
	Band 3	17.8 (13)	19.6	18.0
^{152}Dy	Band 1	17.5 (2)	18.9	17.4

stopping power, and we will defer this discussion to a subsequent publication.

The present data are sufficiently good to draw some conclusions concerning the time history of the side feeding. The best fits to all bands require $(Q_0)_{SF} \approx 15 e b$ in a short cascade of no more than two or three transitions. For the case of the yrast band in ^{149}Gd , where the data are very precise, the fit requires that only one transition be involved. We can state our findings succinctly by noting that the side feeding is equivalent to the decay of a single state with a lifetime approximately equal to that of the observed precursor state. Therefore, this flux is decidedly faster than that coming down the superdeformed band: Indeed, the F values for $^{149}\text{Gd}(1)$ are fit very poorly if the side feeding is not taken into account.

Deformation trajectories in the $(\varepsilon_2, \varepsilon_4)$ plane calculated with the Nilsson-Strutinsky cranking model and the modified oscillator potential with parameters of Ref. [20] are shown in Fig. 2. The previously assigned configurations [1,8–10] are indicated by arrows relating a given band to the ^{152}Dy core. Assuming a sharp uniform charge distribution ρ_0 , contour lines of the macroscopic quadrupole moments,

$$Q_0 = \sqrt{\frac{16\pi}{5}} \frac{\rho_0}{5} \int R^5(\Omega, \varepsilon_2, \varepsilon_4) Y_{20}(\Omega) d\Omega, \quad (2)$$

are drawn with radius parameter $r_0 = 1.2$ fm, and correspond to the nucleus ^{149}Gd . For other nuclei, a scaling factor must be applied. The theoretical values of Q_0 for

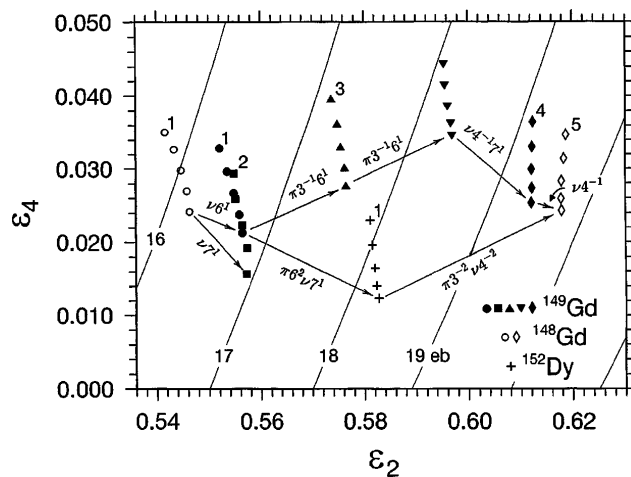


FIG. 2. Calculated deformation trajectories in the $(\varepsilon_2, \varepsilon_4)$ plane for various SD bands. The deformation is shown for spin $I \approx 20\hbar, 30\hbar, 40\hbar, 50\hbar,$ and $60\hbar$, where in all cases ε_4 increases with spin. Contour lines of macroscopic quadrupole moments Q_0 valid for ^{149}Gd (and to a good approximation for ^{148}Gd) are shown. For ^{152}Dy , these contours must be scaled (see text). The arrows show the deformation changes induced by a particle and/or a hole in the following orbitals: $\nu[770]1/2$ ($\nu 7$), $\pi[651]3/2$ ($\pi 6$), $\nu[651]1/2$ ($\nu 6$), $\pi[301]1/2$ ($\pi 3$), and $\nu[411]1/2$ ($\nu 4$). The configurations are taken from [1,8–10]. The deformation trajectory drawn with closed triangles and not labeled by a band number has not been observed to date.

spin $I = 40\hbar$ are listed in Table I together with the experimental values. In general, the calculated values are larger than the measured ones by approximately 10%. Because of uncertainties on the absolute values (stopping powers and r_0 parameter), this discrepancy is not serious, and we have concentrated on relative values using an empirical scaling factor of 0.92 which brings experiment and theory into agreement (Table I).

The yrast SD band of ^{152}Dy has a closed core configuration containing four $N = 6$ protons, two $N = 7$, and eight $N = 6$ neutrons. The yrast SD bands of lighter nuclei are formed by removing particles from these high- N orbitals which are strongly deformation driving. Consequently, we calculate smaller deformations for ^{149}Gd (two $N = 6$ protons and one $N = 7$ neutron removed) and for ^{148}Gd (also one $N = 6$ neutron removed) than for ^{152}Dy . This is seen in Fig. 2, where deformations for these three bands can be read out as $\varepsilon_2 \approx 0.582, 0.555, \text{ and } 0.545$. We note that the calculated changes in ε_4 contribute so as to increase the differences in the quadrupole moment between these configurations. This confirms earlier predictions [21] that at the $\sim 2 : 1$ axis ratio, the shell gaps are not fixed at a specific particle number and deformation. Instead, there are broad regions of low level density in the range of ε_2 between 0.5 and 0.6, where the favored particle numbers increase with increasing deformation.

Starting from ^{152}Dy , we can remove particles in up-sloping equatorial orbitals, making configurations assigned to *excited* bands in lighter nuclei. The most extreme case is $^{148}\text{Gd}(5)$, where two $[301]1/2$ protons and two $[411]1/2$ neutrons are removed. This leads to deformation changes of a similar magnitude to those encountered in down-sloping orbitals but now in the opposite direction. For example, we predict a very large deformation $\varepsilon_2 \approx 0.618$ for $^{148}\text{Gd}(5)$ which is much larger than that of the yrast band, $^{148}\text{Gd}(1)$. Overall, the agreement with theory shown in Table I is remarkably good. The most serious discrepancy is for $^{149}\text{Gd}(3)$, where relative to $^{149}\text{Gd}(1)$, a proton has been excited from an up-sloping $[301]1/2$ orbital to a down-sloping $N = 6$ orbital. The change in deformation predicted is not observed, but the discrepancy is within the uncertainties.

A vital issue is whether IBs (bands with identical $J^{(2)}$ moments of inertia) have the same deformation. In the present data, $^{148}\text{Gd}(5)$ and $^{149}\text{Gd}(4)$ are identical to $^{152}\text{Dy}(1)$, and their quadrupole moments are equal within the uncertainties. Nevertheless, this does not mean that they have the same deformation. The macroscopic quadrupole moment scales according to $ZA^{2/3}$, and this factor changes by 5% between ^{148}Gd and ^{152}Dy (but only by 0.5% between ^{148}Gd and ^{149}Gd). Consequently, although the calculated deformation is smaller in ^{152}Dy than in the IBs of ^{148}Gd and ^{149}Gd , we obtain similar quadrupole moments (Fig. 2 and Table I). The conclusion that the deformation could be different in bands with identical $J^{(2)}$ moments supports the analysis of Ref. [22]. There it was found that the effect on $J^{(2)}$ from defor-

mation changes caused by the extra particle and from the alignment (difference in spin between the two bands at a constant rotational frequency) brought in by this particle are not negligible, but their effects on $J^{(2)}$ cancel in IBs.

In summary, we have measured accurate lifetimes in SD bands of $^{148-149}\text{Gd}$ and ^{152}Dy nuclei. Differences in the observed yrast band quadrupole moments are nicely explained in terms of the different occupation of high- N orbitals. Furthermore, the present results indicate that alignment effects and deformation changes tend to compensate in identical bands. The calculations also predict small shape changes as a function of spin. This is the case both in the macroscopic calculations presented here and in the microscopic ones of Ref. [1]. Our data neither support nor exclude such deformation changes, and it will be an important goal of future experiments to test this prediction.

Eurogam is funded jointly by the EPSRC (U.K.) and IN2P3 (France). This work was supported by EPSRC (U.K.), SNSRC (Sweden), NSERC (Canada), AECL (Canada) and KBN-2P03b112, KBN-12108 (Poland).

-
- [1] T. Bengtsson, S. Åberg, and I. Ragnarsson, Phys. Lett. B **208**, 39 (1988).
 - [2] W. Nazarewicz, R. Wyss, and A. Johnson, Nucl. Phys. **A503**, 285 (1989).
 - [3] M. A. Bentley *et al.*, Phys. Rev. Lett. **59**, 2141 (1987).
 - [4] B. Cederwall *et al.*, Nucl. Instrum. Methods Res., Sect. A **354**, 591 (1995).
 - [5] B. Haas *et al.*, Phys. Rev. Lett. **60**, 503 (1988).
 - [6] P. Fallon *et al.*, Phys. Lett. B **257**, 269 (1991).
 - [7] C. Baktash, B. Haas, and W. Nazarewicz, Annu. Rev. Nucl. Sci. **45**, 485 (1995).
 - [8] S. Flibotte *et al.*, Nucl. Phys. **A584**, 373 (1995).
 - [9] G. de Angelis *et al.*, Lawrence Berkeley Laboratory Report No. LBL-35687, 1994 (unpublished).
 - [10] G. de France, Proceedings of the International Spring Seminar on Nuclear Physics, New Perspectives in Nuclear Structure, Ravello, Italy, 1995 (to be published).
 - [11] F. A. Beck, Lawrence Berkeley Laboratory Report No. LBL-35687, 1994 (unpublished).
 - [12] L. C. Northcliffe and R. F. Schilling, Nucl. Data Tables **7**, 256 (1970).
 - [13] S. H. Sie *et al.*, Nucl. Phys. **A291**, 443 (1977).
 - [14] J. Lindhard, M. Scharff, and H. E. Schiott, Mat. Fys. Medd. K. Dan. Vidensk. Selsk. **33**, No. 14 (1963).
 - [15] K. B. Winterbon, Atomic Energy of Canada Limited Report No. AECL-3194, 1968 (unpublished).
 - [16] A. E. Blaugrund, Nucl. Phys. **88**, 501 (1966).
 - [17] J. C. Bacelar *et al.*, Phys. Rev. C **35**, 1170 (1987).
 - [18] J. Gascon *et al.*, Nucl. Phys. **A513**, 344 (1990).
 - [19] J. F. Ziegler, J. P. Biersack, and U. Littmark, *The Stopping and Range of Ions in Solids* (Pergamon, New York, 1985).
 - [20] B. Haas *et al.*, Nucl. Phys. **A561**, 251 (1993).
 - [21] I. Ragnarsson, S. G. Nilsson, and R. K. Sheline, Phys. Rep. **45**, 1 (1978).
 - [22] I. Ragnarsson, Nucl. Phys. **A520**, 67c (1990).